Kalaiselvi et al., J Biotechnol Biomater 2017, 7:4
DOI: 10.4172/2155-952X.1000275

Journal of Biotechnology & Biomaterials

Research Article Open Access

Sol-Gel Mediated Synthesis of Pure Hydroxyapatite at Different Temperatures and Silver Substituted Hydroxyapatite for Biomedical Applications

Kalaiselvi V[1,2]*, Mathammal R[3], Anitha P[4]

[1]Research scholar, Sri Sarada college for women Salem
[2]Department of Physics, Navarasam arts &Science College for Women, Arachalur, Erode.638101
[3]Department of Physics, Sri Sarada College for women, Salem, Tamil Nadu, India
[4]Department of Physics, Vellalar College for women, Erode, Tamil Nadu, India

Abstract

Owing to excellent bio compatibility and bioactivity of Hydroxyapatite (HAP), it plays a vital role in the field of medicine such as orthopaedic and dental applications. In the present work sol- gel method of synthesizing nano Hydroxyapatite using Calcium hydroxide as calcium source and Orthophosphoric acid as Phosphorus source and maintain the Ca:P ratio as 1:67. The synthesized samples are calcined under different temperature ranging from 400 to 700°C. The crystalline size of the synthesised samples are calculated using X-ray diffraction (XRD), Morphology of the surface by scanning electron microscope (SEM) and (TEM), existence of functional groups were revealed by Fourier transformation IR spectroscopy (FTIR). Thus the studies suggest that the Hydroxyapatite calcined at high temperatures is the best biomaterial for dental applications. Then it was substituted with silver and further studied with XRD, SEM, EDAX, FTIR, TEM, antimicrobial activity.

Keywords: Sol-gel method; Calcination; Silver; Antimicrobial

Introduction

Hydroxyapatite is the biomaterial and mineral component of bone [1,2]. Bone is the only organ that provides basic mechanical support to the body. It generates and transfers the locomotive forces [3]. Bone consist of approximately 8 wt% water, 22 wt% protein and 70 wt% minerals [4]. The mineral component of the bone appears in the form of calcium phosphate [5] which is the main mineral reservoir for the body. Among all biomaterials calcium phosphate attracts the researchers due to its excellent biocompatibility and its non- toxicity. G It is a very good drug delivery carrier, biodegradable, biocompatible, less soluble. Calcium phosphate has the Ca:P molar ratio ranges from 1.57 to 1.77. The system with this ratio are less soluble in blood and is supersaturated. Calcium phosphate exists in different forms according to Ca:P ratio such as hydroxyapatite, octa-calcium phosphate, tri-calcium phosphate, di-calcium phosphate dehydrate and di-calcium phosphate. The bones major 65% weight is accounted by Hydroxyapatite which has the hexagonal crystalline structure supplies strength and stiffness to bone [5]. Hydroxyapatite crystals appear in the form of rod like structure in bone with a size ranges less than 100 nm [6]. Also this hydroxyapatite has excellent biocompatible and osteoconductive nature [7]. The research deals with pure at different temperatures and silver incorporation at 700°C calcined sample.

The preparation of hydroxyapatite powder with controlled morphology, stoichiometry crystallinity and crystallite size in nano range is predominant in the production of biomaterials. The hydroxyapatite bio ceramic has poor mechanical properties. Hydroxyapatite has high bioactivity; nontoxic with much medical application in porous dense and granule forms [8]. Different synthesizing techniques for hydroxyapatite are in progress for the recent years. These techniques are sol-gel method, controlled precipitation [9], wet chemical [10], spray pyrolysis [11], hydrothermal synthesis [12], mechano-chemical method [13] and microwave method [14]. Among all sol gel method has gained much attention due to inherent advantages namely low temperature process, homogeneity, molecular mixing, able to produce nano crystalline powders with high purity. This route can be used to produce very sophisticated nanomaterial and to tailor the materials to very specific applications [15].

The stability, contact at natural and artificial bone interface is the best parameter of nanosized sol gel product. The present work was aimed to synthesize Hydroxyapatite Nanoparticles at different temperature ranging from 400°C to 700°C and determine the crystallite size by X-Ray diffraction method (XRD), structural morphology by scanning electron microscope (SEM) and functional groups by Fourier transform IR spectroscopy (FTIR).

Silver and silver based materials are antimicrobial and disinfectant material; it exhibits low toxicity, biocompatibility, stability and antimicrobial activity. Hydroxyapatite is brittle in nature and to improve load bearing capacity it is further substituted with metals. Silver is the best material for medical applications. Extent of silver substitution for calcium ions is made. Ratio is maintained as (Ca+Ag)/P to be 1.67. The ratio of silver and calcium are maintained as (0.9+0.1). Further its characteristics are studied via XRD, SEM, EDAX, FTIR, TEM, Antimicrobial activity.

Experimental Sections

Materials utilized

All the chemicals were used of analytical grade available from commercial sources. Calcium hydroxide 99% sigma Aldrich, Orthophosphoric acid 98% Sigma Aldrich, Silver Nitrate 98% Sigma Aldrich, Ammonia solution was procured and utilized without further purification.

***Corresponding author:** Kalaiselvi V, Department of Physics, Navarasam Arts and Science College for Women, Arachalur, Erode 638101, India, Tel: +919789111334; E-mail: nk.arthikalai@gmail.com

Received September 08, 2017; **Accepted** October 19, 2017; **Published** October 26, 2017

Citation: Kalaiselvi V, Mathammal R, Anitha P (2017) Sol-Gel Mediated Synthesis of Pure Hydroxyapatite at Different Temperatures and Silver Substituted Hydroxyapatite for Biomedical Applications. J Biotechnol Biomater 7: 275. doi: 10.4172/2155-952X.1000275

Methods of synthesis

Synthesis of pure hydroxyapatite: Calcium hydroxide and Orthophosphoric acid are the host precursors for calcium and phosphorous. 1 M of calcium hydroxide and 0.6 M of orthophosphoric acid were prepared using double distilled water and it was stirred for 30 min, separately. The orthophosphoric acid solution was added in drops to the calcium hydroxide solution. After adding it the precipitated solution was vigorously stirred for an hour. The pH of 11 was maintained by the addition of ammonia solution drop wise. The solution was aged for 24 h. The precipitate was dried in oven for 6 h less than 200°C. Thus made product was placed in furnace at different temperatures ranging from 400°C-700°C for 3 h. The powders calcined at 400°C was labelled as HAP 1, 500°C as HAP 2, 600°C as HAP 3 and 700°C as HAP 4.

Synthesis of silver substituted hydroxyapatite: Calcium hydroxide and Orthophosphoric acid are the precursors for calcium and phosphorous. 0.9 M of calcium hydroxide and 0.6 M of orthophosphoric acid were prepared using double distilled water and it was stirred for 30 min separately. 0.1 M Silver nitrate solution was added drop wise and made to stir for 2 h. Further orthophosphoric acid solution was added in drops. After adding it the precipitate was vigorously stirred for 1 h. The pH of 11 was maintained by the addition of ammonia solution drop wise. The solution was aged for 24 h. The precipitated solution was dried in oven for 6 h less than 200°C and calcined in furnace for 2 h. The sample is named as HAP5.

Characterization techniques

X-Ray diffraction method: All the synthesized samples are characterized by X-Ray diffraction (XRD) analysis. 20 to 80°C is the 2θ range of recorded data. The XRD determines the crystallite size and crystallinity were carried out using the XRD pattern obtained.

The Debye Scherer formula is used to determine the average particle Crystallite size from XRD pattern from the line broadening measurement.

$$D = \frac{0.89\lambda}{\beta cos\theta}$$

Where The X-ray wavelength is λ.

The full width at half maximum of Hydroxyapatite line is β and the diffraction angle is denoted by θ.

The crystallinity degree of the calcined powders was calculated by

$$X_c = 1 - \frac{V_{\frac{112}{300}}}{I_{300}} \wedge$$

Where intensity of (300) reflection of Hydroxyapatite is $I_{300,}$ Intensity between (112) and (300) reflections is $V_{112/300.}$

FT-IR spectroscopy: Fourier transform infrared spectroscopy analysis reveals the functional groups which are recorded in the 4000-400 cm^{-1} region.

Scanning electron microscopy with EDAX: The morphology of surface in the calcined Hydroxyapatite samples at different temperatures were studied using Scanning Electron Microscopy. The stoichiometry of the samples was studied by EDAX.

Transmission electron microscopy: TEM is useful to observe morphology, crystal orientation, electronic structure and particle size. The morphology and size of the particles in the prepared sample was analyzed using JEOL JEM-2100 transmission electron microscope with different magnification.

Antimicrobial activity: The strains of *Pseudomonas aeruginosa* and *Bacillus subtilis* were studied. The bacteria's were grown overnight by adding Yeast solution and centrifuged with Phosphate buffered saline solution. The samples are placed in the beaker with the addition of the prepared bacteria and incubated for 24 h. The colony forming units are visually counted.

Results and Discussion

The formation of Hydroxyapatite during the sol gel method can be expressed by the relation:

$$10Ca(OH)_2 + 6H_3PO_4 \rightarrow Ca_{10}(PO_4)_6(OH)_2 + 18H_2O$$

Water can be removed as by product on centrifuging.

X-ray diffraction

Figure 1 compares the XRD pattern of Hydroxyapatite phase evolution from 400 to 700°C (HAP1, HAP2, HAP3, HAP4). All spectra show only Hydroxyapatite reflection. As per the JCPDS card no. 09-0432 the powders are hexagonal and are well matched. The crystallinity of Hydroxyapatite increases with the increase in temperature. The crystallinity and crystalline size of the samples calcined at different

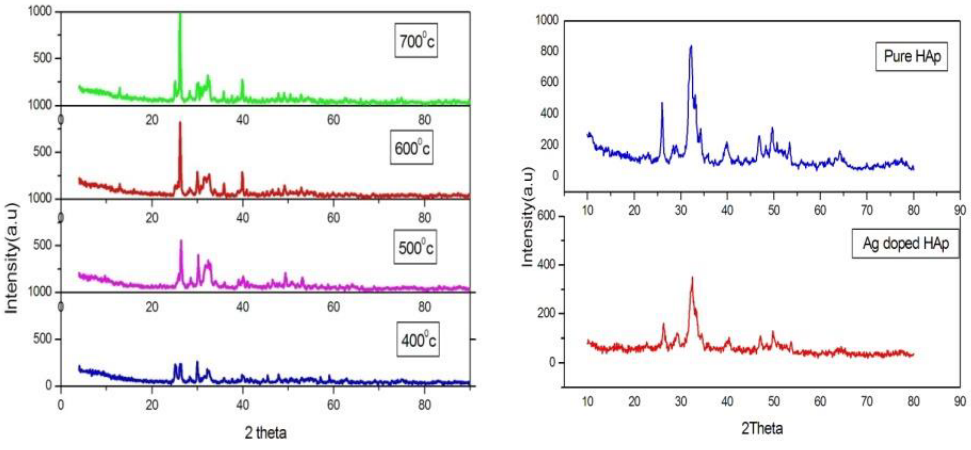

Figure 1: XRD pattern of pure Hapand Ag doped Hap.

temperature was determined using Debye Scherer equation and displayed in the Table 1. The crystallite size is calculated by considering three high intensity peaks (002), (211) and (222).These three peaks are well matched with JCPDS value hence these are chosen for calculation. Average mean crystallite size of all samples was displayed in the Table 1. 10 nm, 17 nm, 35 nm and 57 nm are the crystallite size of HAP1, HAP2, HAP3, HAP4, respectively. The crystallite size decreases with increase in temperature. No activity on bioresorption was shown on Hydroxyapatite calcined at higher temperature [16]. Hydroxyapatite is insoluble in other solutions which avoids corrosion resistance of teeth in saliva at different pH values [17,18]. Crystallinity of hydroxyapatite founds to be increased from 10 nm to 57 nm respectively in the calcinations at 400°C to 700°C. We can observe clear increase in intensity at raise of temperature. Also the resolutions of the XRD peaks are enhanced with increase in temperature. Each sample was calcined for 3 h. The reason for calcinations for 3 h proves that there is no change in the XRD peaks as the calcined time increases.

S. No.	Sample	Crystallite size (nm)	Degree of Crystallinity
1	HAp1	10	0.266
2	HAp2	17	0.458
3	HAp3	35	0.808
4	HAp4	57	0.861
5	HAp5	57	0.869

Table 1: Average mean crystallite size of all samples using Debye Scherer equation.

Sample	2θ	d spacing	h	k	l	a=b (A^0)	C (A^0)
HAp	25.87	3.44	0	0	2	-	6.88
	32.9	2.72	3	0	0	9.4224	-
	51.28	1.78	4	1	0	9.4189	
	53.14	1.72	0	0	4		6.888
Average						9.4206	6.884
Ag-HAp	26.29	3.3867	0	0	2		6.8694
	32.49	2.753	3	0	0	9.4454	
	49.98	1.8231	4	1	0	9.4288	
	53.4	1.7143	0	0	4		6.8535
Average						9.4371	6.8614

Table 2: The 2θ values, hkl values [22] and Lattice constants (a, c) of pure and Ag doped HAp.

The sharp and narrow peaks insist the good crystallinity of the samples. A slight shift in the peaks of Ag Hap (HAp5) is found in pure HAp (HAp1-HAp4) due to the substitution of silver in HAp. The 2θ values for the HAp peaks and its hkl values [19] and Lattice constants (a, c) of pure and Ag doped HAp (HAp5) were displayed in Table 2.

Fourier transform infrared spectroscopy

Figure 2 compares the FTIR spectra of the calcined samples ranging from 400°C to 700°C. The bands at 1650 cm^{-1} is the bending mode of H_2O in hydroxyapatite at 400°C and 500°C compared to hydroxyapatite at 600°C and 700°C. The stretching vibration of the phosphate group was revealed in the presence of two characteristic bands at 1033 cm^{-1} and 1095 cm^{-1}. The OH^- bending mode in hydroxyapatite lattice is due to the characteristic peaks at 601 cm^{-1}.The bands at 563 and 470 cm^{-1} corresponding to PO_3 group which is present at calcined samples.

After the heat treatment no peaks related to CO_3^{2-} group that is 1420 cm^{-1} was not detected. Synthesis of hydroxyapatite is revealed by the absence of large peaks located at 3550 cm^{-1} assigned for water molecules. The absorption bands at 3581 cm^{-1}, 3561 cm^{-1}, 3487 cm^{-1}, 2430 cm^{-1}, 1283 cm^{-1} and 917 cm^{-1} show that octacalcium phosphate is absent and this confirms the stoichiometry of hydroxyapatite [20,21]. The bands corresponding to hydroxyl group decreases as the temperature increases. The strength of PO_4^{3-} stretching vibration peaks is increased in Hydroxyapatite as calcination temperature increases. This was revealed by the FTIR spectra of nano hydroxyapatite calcined at different temperature from 400°C to 700°C (HAp1-HAp4). We found a slight shift in the FTIR of Ag doped HAp (HAp5) which is predicted in the Figure 2.

Scanning electron microscope analysis with EDAX

The morphologies of the prepared powders calcined under different temperature ranging from 400 to 700°C (HAP1-HAP4) were observed by SEM are shown in Figure 3. These samples consist of particles with

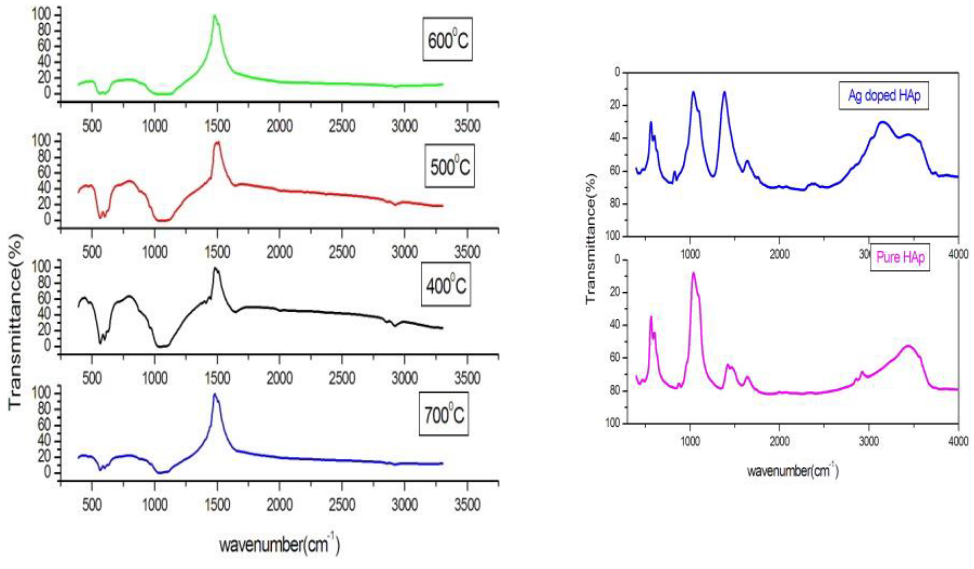

Figure 2: FTIR spectra of pure HAp and Ag doped Hap.

fine grain, homogeneous and uniform distribution of components. SEM images show the morphological nano rod like structures which are similar to that of human teeth morphology. Width and length of the nano rods are in the range of 47 to 155 nm and 240 to 878 nm varies for different temperatures. From the results it was revealed that length and width of nano rods changes as the temperature increases. This means when temperature increases the OH^- concentration decrease, which results in increase in length of the nano rod. When temperature increases there was a rod shaped morphology in the sample. Ag doped HAp shows spherical shaped morphology in the image. Figure 4 displays the images of EDAX. The stoichiometric ratio of Pure and Silver substituted samples by EDAX was revealed in the Table 3.

Transmission electron microscope analysis

The Figure 5 reveals the transmission electron microscopy of silver doped HAp. The figure reveals needle or rod shaped morphology of the sample at lower and higher magnification. The composite analysis predicts that both the samples match well with standard shape and morphology.

Antimicrobial activity

The antibacterial activity of ciprofloxacin loaded HAp against the gram positive cocci *Bacillus subtilis* and gram negative bacilli *Pseudomonas aeruginosa* by agar well diffusion method was studied. The surface area of the nanoparticles increases and forms bonds with the microorganisms and causes death of cells. A microorganism membrane causes structural changes, regulates transport through membrane causing death finally. The Zone of inhibition is tabulated. Silver doped samples exhibit more zone of inhibition due to its antibacterial property [22,23]. Figure 5 (VK1) and 6 (VK2) reveals good zone of inhibition for positive cocci *Bacillus subtilis* and negative bacilli *Pseudomonas aeruginosa* in pure HAp and Ag doped Hap [24] respectively. Tables 4 and 5 reveals the presence of Zone of inhibition of pure HAp (HAp4) and Ag doped HAp (HAp5), respectively. Ciproflaxcin shows more zone of inhibition compared to samples due to its standard antimicrobial property. HAp5 possess good Zone of inhibition because of silver substitution.

Sample	Ca	P	Ca/P
Pure HAp	12.13	7.21	1.68
Ag doped HAp	23.81 (Ca: 22.26, Ag:1.55)	13.31	1.77

Table 3: The stoichiometric ratio of pure and silver substituted samples revealed by EDAX.

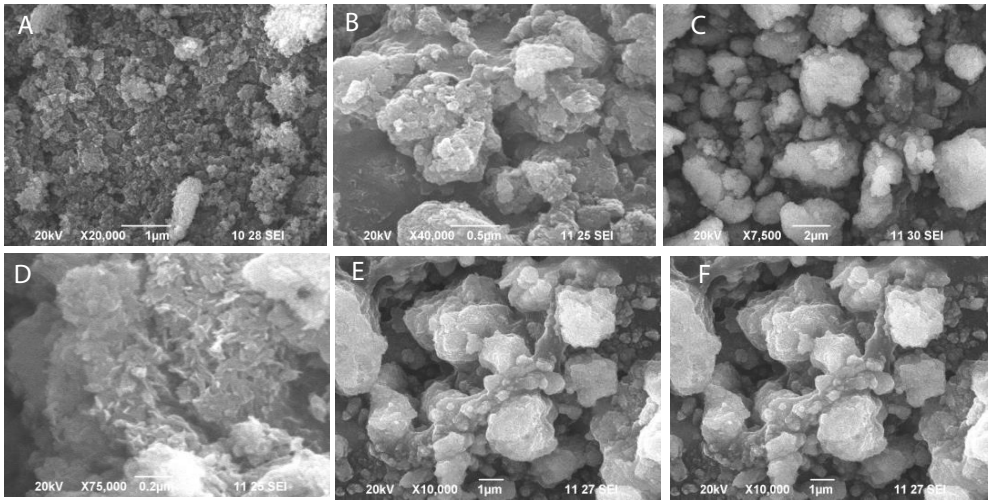

Figure 3: Scanning electron microscope analysis of pure HAp and silver doped Hap.

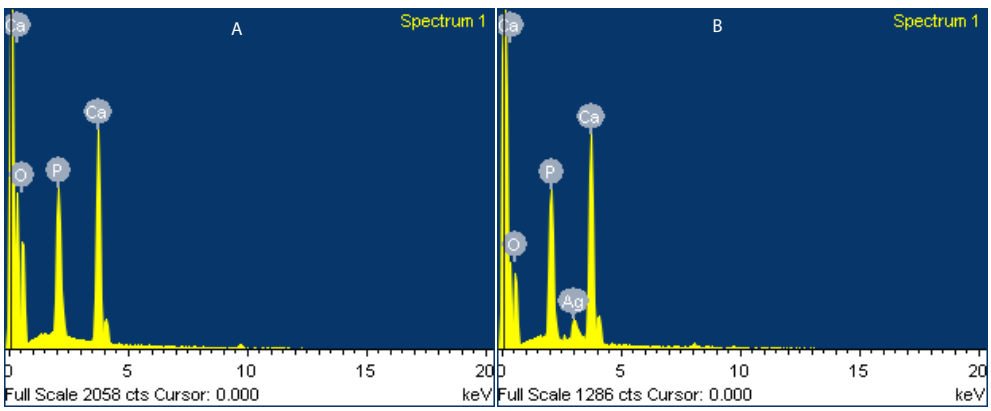

Figure 4: EDAX images of pure HAp and Ag doped HAp.

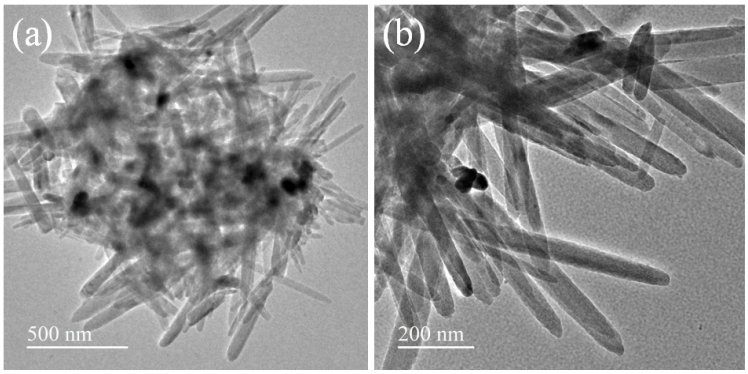

Figure 5: TEM images of Ag doped HAp.

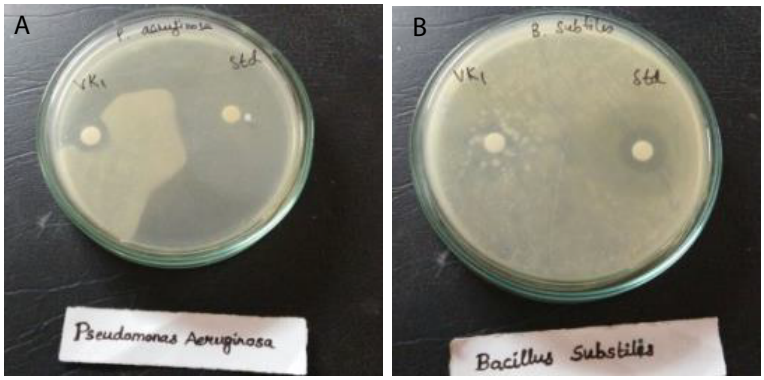

Figure 6: Antimicrobial activity of bacteria's of pure HAp.

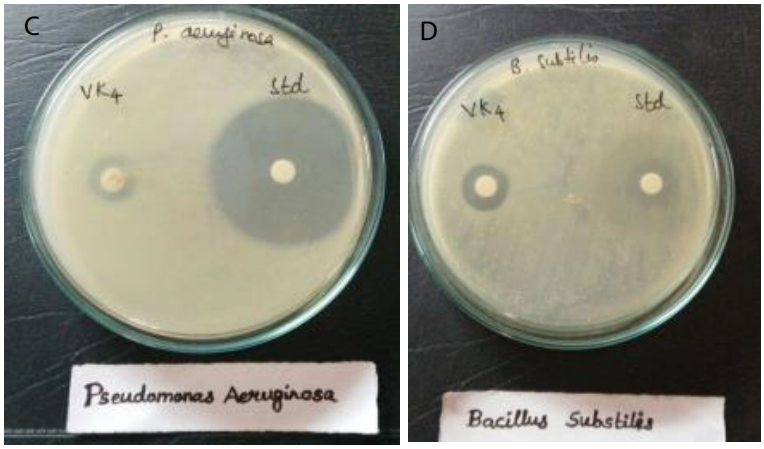

Figure 7: Antimicrobial activity of two bacteria's for Ag doped Hap.

S. No.	Organisms	Zone of Inhibition (mm)	
		Std Ciprofloxacin (10 µg/disc)	Sample (100 µg/ disc)
1	*Bacillus subtilis*	33	9
2	*Pseudomonas aeruginosa*	42	14

Table 4: Zone of inhibition of Pure HAp against *Bacillus subtilis* and *Pseudomonas aeruginosa.*

S. No.	Organisms	Zone of Inhibition(mm)	
		Std Ciprofloxacin (10 µg/disc)	Sample (100 µg/disc)
1	*Bacillus subtilis*	30	14
2	*Pseudomonas aeruginosa*	42	16

Table 5: Zone of inhibition of silver doped HAp against *Bacillus subtilis* and *Pseudomonas aeruginosa.*

Conclusion

The synthesis and calcinations of nano hydroxyapatite through Sol gel process by varying the calcinations temperatures using the precursor's calcium hydroxide and orthophosphoric acid was investigated using XRD, FTIR and SEM. XRD investigation reveals that the crystallite size, crystallinity increases with the increase in temperature ranging from 400°C to 700°C. FTIR studies enumerated all the characteristic bands of hydroxyapatite. SEM and TEM study reveals the formation of nano rods which stimulates the surface morphology, particle size and phase purity of hydroxyapatite in human tooth. EDAX predicts the composition of the samples which matches 1.6 for pure HAp (HAp1-HAp4) and 1.7 for Ag doped HAp (HAp5). Antimicrobial studies show good zone of exhibition in (HAP4&5) both the samples. Thus the studies suggest the hydroxyapatite calcined at high temperatures (HAp4) is best biomaterial in dentistry and silver doped samples (HAp5) are good candidates in the field of medicine.

References

1. Haresh MP (2012) Modelling scenario in nanotechnology today. J Environ Nano Tech 1: 01-04.
2. Amin Shavandi, Alaa El DA, Azam A, Zhifa S (2015) Synthesis of nano-hydroxyapatite (nHA) from waste mussel shells using a rapid microwave method. Mat Chem Phy 149: 607-616.
3. Tathe A, Pratimanikalje A (2010) A brief review: Biomaterials and their application. Int J Pharm Pharm Sci 2: 19-23.
4. Sahil J, Cuneyt T, Sarit BB (2004) Microwave assisted synthesis of calcium phosphate nanowhiskers, J Mater Res 19: 1876-1881.
5. Haded A, Jeffrey LE (2011) Preparation of nanostructured hydroxyapatite in organic solvents for clinical application. Trends Biomat Artif Org 25: 12-19
6. Kapoor S, Batra U, Kohli S (2011) Transformation in sol-gel synthesized nanoscale Hydroxyapatite calcined under different temperatures and Time conditions, J Mat Eng perf 21: 1738-1743.
7. Sanosh KP, Min C, Balakrishnan A, Kim TN, Seong Jai Cho (2009) Preparation and characterization of nano hydroxyapatite powder using solgel technique. Bull Mate Sci 32: 465-470.
8. Sopyan I, Nawawi NA (2011) Sintering and properties of dense manganese doped calcium phosphate bio ceramics prepared using sol-gel derived nanopowder. Mater Manufac Process 26: 908-914.
9. Mark IJ, Haneen B, Darrell AP (2002) Production of hydroxyapatite from waste mussel shells. Mater Sci Eng, pp: 18-19.
10. Haresh M, Pandya P (2013) Comprehensive review of preparation methodologies of nano hydroxyapatite. J Environ Nanotechnol 3: 101-121.
11. Gobi D, Indira J, Nithiya S, Kavitha L, Kmchi Mudali U (2013) Influence of surfactant concentration on nano hydroxyapatite growth. Bull Mater Sci 36: 799-805.
12. Koumoulidis GC, katsoulidis AP (2003) Preparation of hydroxyapatite via micro emulsion route. J Colloid Interf Sci 259: 254-260.
13. Kanchana P, Sekar C (2014) EDTA assisted synthesis of hydroxyapatite nanoparticles for electrochemical sensing of uric acid. Mater Sci Eng 42: 601-607.
14. Kalaiselvi V, Mathammal R (2015) Effect of titanium dioxide doping on nano hydroxyapatite synthesized from egg shells via wet chemical method. Int J Magaz Eng Technol 3: 133.
15. Uskokovic K, Uskokovic DP (2010) Nano sized hydroxyapatite and other calcium phosphates: Chemistry of formation and application as drug and gene delivery agents. J Biomed Mater Res B 96:152-191.
16. Temenoff JS, Mikos AG (2008) Biomaterials: The intersection of biology and materials science. Prentice Hall, New Jersey.
17. Ratner BD, Hoffman AS, Schoen FJ, Lemons JE (2004) An introduction to naturals in medicine. Elsevier Academic Press, San Diego.
18. Aoki H (1991) Science and medical application of Hydroxyapatite. Japanese Association of Apatite Science, Tokyo, Japan.
19. Mavis B, Tas AC (2000) Dip coating of calcium hydroxyapatite on Ti-6Al-4v substrate, J Am Cer Soc 83: 989-991.
20. Anna S, Zofia P (2005) FTIR and XRD evaluation of carbonated hydroxyapatite powders synthesized by wet method. J Mol Struct 744: 657-661.
21. Suchanek W, Yoshimura M (1998) Processing and properties of hydroxyapatite based biomaterials for use as hard tissue replacement implants. J Mater Resour 13: 94-117.
22. Lim GK, Wang J (1999) Formation of nanocrystalline hydroxyapatite in non-ionic surfactant emulsion. Langmuir 15: 7472-7477.
23. Padmanabhan SK, Balakrishnnan A, Chu MC, Lee YJ, Kim TN (2009) Sol-gel synthesis and characterization of hydroxyapatite nanorods. Particuology 7: 466-470.
24. Rameshbabu TS, Sampathkumar TG, Prabhakar VS, Sastry KV, Murty GK, et al. (2006) Antibacterial nanosized silver substituted hydroxyapatite: Synthesis and characterization. J Biomed Mat 80: 581-590.